



Published in final edited form as:

Mol Pharm. 2012 March 5; 9(3): 374–381. doi:10.1021/mp2003219.

## Preparation of Cystamine Core Dendrimer and Antibody-dendrimer conjugates for MRI Angiography

Kido Nwe, Diane E. Milenic, Geoffrey L. Ray, Young-Seung Kim, and Martin W. Brechbiel  
Radioimmune & Inorganic Chemistry Section, Radiation Oncology Branch, National Cancer Institute, 10 Center Drive, Bethesda, MD 20892

### Abstract

We herein report the preparation along with the *in vivo* and *in vitro* MRI characterization of two generation four and five cystamine core dendrimers loaded with thirty and fifty-eight derivatized Gd-DOTA (G4SS30, G5SS58) respectively. Likewise the development and characterization of two half-dendrimers conjugated to the F(ab')<sub>2</sub> fragment of the monoclonal antibody (mAb) panitumumab functionalized with a maleimide conjugation functional group site (Ab-(G4S15)<sub>4</sub>, Ab-(G5S29)<sub>4</sub>) are also described. The *in vitro* molar relaxivity of the Ab-(G4S15)<sub>4</sub> conjugate, measured at pH 7.4, 22°C, and 3T showed a moderate increase in relaxivity as compared to Magnevist (6.7 vs. 4.0 mM<sup>-1</sup>s<sup>-1</sup>) while the Ab-(G5S29)<sub>4</sub> conjugate was two-fold higher (9.1 vs. 4.0 mM<sup>-1</sup>s<sup>-1</sup>). The data showed that only a high injection dose (0.050 mmol Gd<sup>3+</sup>/kg) produced a detectable contrast enhanced contrast for the Ab-(G4S15)<sub>4</sub> conjugate while a lower dose (0.035 mmol Gd<sup>3+</sup>/kg) was sufficient for the Ab-(G5S29)<sub>4</sub> conjugate. The antibody-SMCC conjugate was purified by a Sephadex G-100 column and the antibody-dendrimer-based agents were purified by spin filtration using a Centricon filter (50,000 MCO). The protein assay coupled with Cysteine and Ellman's assay indicated an antibody to dendrimer ratio of 1:4. The *in vivo* blood clearance half-lives of the four agents measured at the jugular vein were ~12-22 min.

### Introduction

Magnetic resonance imaging (MRI) possesses a unique property of being non-invasive, and thus is a widely used imaging modality for both diagnosis and biomedical research. In most applications synthetic contrast agents, such as [Gd(DTPA)(H<sub>2</sub>O)]<sup>-2</sup> (Magnevist®), are employed to induce more contrast and thus increase the sensitivity of the MRI scan.<sup>1</sup> These low molecular weight contrast agents rapidly extravasate from the blood vessels into interstitial spaces and rapidly decrease in concentration from the blood vessels prompting the development of new and efficient agents. The most well known strategy to obviate these problems is to increase the molecular size of the agent which is accomplished by conjugation of a small molecule MRI contrast agent to a larger macromolecule such as a dendrimer or protein to prolong the intravascular retention time. The relaxation efficiency of water protons in contact with the contrast agent is also altered by the concomitant decrease in the molecular tumbling time, also known as rotational correlation time  $\tau_r$ .<sup>2-3</sup> The use of small Gd(III) chelates conjugated to high molecular weight carriers such as mono-dispersed polyamidoamine (PAMAM) dendrimers, which possess a large number of available amine surface groups for conjugation, is well documented.<sup>4-6</sup> PAMAM dendrimers with defined structure have found uses for conjugation of high numbers of small molecule contrast agents for MRI,<sup>6-9</sup> as well as monoclonal antibodies for directed targeting.<sup>10-13</sup>

There is a continuing interest in the application of mAb to develop targeted molecular MRI agents for both diagnostic as well as for therapeutic purposes. Antibody-dendrimer conjugates have been explored for use in radioimmunotherapy and imaging applications, including MRI, with promising outcomes.<sup>13-16</sup> The principle of conjugation of dendrimer to

protein through maleimide-thiol conjugation chemistry, either using the succinimidyl 4-[N-maleimidomethyl]cyclohexane-1-carboxylate (SMCC) bridge<sup>17</sup>, or biotin (Maleimide-PEO<sub>2</sub>-biotin)<sup>18</sup> have been demonstrated previously. Disulfide core-linked dendrimer (cystamine core) scissions in half upon reduction via redox chemistry resulting in a unique thiol terminal group that can site specifically react with a maleimide, which makes it a very attractive building block to assemble dendrimer-protein, -peptide, or other targeting vector conjugates.

Panitumumab, a fully human mAb, was approved by the U.S. Food and Drug Administration (FDA) in 2006 and is indicated for the treatment of epidermal growth factor receptor (EGFR)-expressing metastatic colorectal cancer.<sup>19-20</sup> Panitumumab has been demonstrated to have benefit for cancers of the colon, lung, pancreas, prostate, ovary and others<sup>21</sup> Studies from this laboratory have further shown the utility of this mAb, when radiolabeled, for imaging and therapeutic procedures, expanding the potential patient population that would benefit from this EGFR targeting mAb.<sup>22</sup> For purposes such as imaging, the intact mAb may not be the most suitable form of the molecule. Fragments such as the F(ab')<sub>2</sub> of mAb have been shown to have more favorable properties, i.e., faster blood clearance, shorter whole body residence time and greater tumor penetration, which result in lower background signal or noise and thus enhance image contrast.<sup>23-25</sup>

The present study reports the preparation and preliminary assessment of panitumumab monoclonal antibody-dendrimer (mAb-Den) conjugates for use as intravascular contrast agents. To demonstrate the viability of the method, the pre-formed complex, (2-(4-isothiocyanatobenzyl)-1,4,7,10-tetraazacyclododecane-*N,N',N'',N'''*-tetraacetic acid gadolinium complex C-DOTA-Gd, was directly conjugated to the cystamine core generation 4 and 5 dendrimers. The dendrimers were then reduced using a disulfide reducing gel and conjugated to a maleimide group functionalized of panitumumab F(ab')<sub>2</sub>. The ultimate goal is to utilize these mAb-Den agents for site specific imaging, and the smaller F(ab')<sub>2</sub> fragment was chosen as the vehicle for targeting of the antigen. The impact of the agents on water proton relaxation was studied comparatively *in vitro* whereas their performance as contrast agents was studied *in vivo*.

## Experimental

### Materials and methods

Cystamine core Starburst® polyamidoamine (PAMAM) dendrimer generations 4 and 5 (G4SS and G5SS from this point on) in MeOH were obtained from Dendritic Nanotechnologies, Inc. The F(ab')<sub>2</sub> fragment of panitumumab was produced as previously described.<sup>23</sup> Gadolinium nitrate pentahydrate (Gd(NO)<sub>3</sub>·5H<sub>2</sub>O) was purchased from Aldrich (St. Louis, MO). Phosphate buffered saline (PBS) at pH 7.4 was obtained from Digene (Gaithersburg, MD). Size-exclusion HPLC (SE-HPLC) was performed using a Beckman System Gold® (Fullerton, CA) equipped with a model 126 solvent delivery module and a model 166NMP UV detector ( $\lambda$  254 nm) controlled by 32 Karat software. A TSK-gel G3000SWxl 10  $\mu$ m, 7.8 mm  $\times$  300 mm column and a TSK-gel 10  $\mu$ m guard column (Tosoh Bioscience, Montgomeryville, PA) were used for SEHPLC with PBS as the eluent at 1.0 mL/min, respectively. All water used was purified using a Hydro Ultrapure Water Purification system (Rockville, MD). The Sephadex® G-50 and 100 resins were purchased from Pharmacia (Sweden), pre-treated with PBS, and loaded into a Pharmacia Biotech column (Uppsala, Sweden) 1.0  $\times$  21.2 cm for G-100 and 2.6  $\times$  39.7 cm for G-50. Elemental analyses were performed by Galbraith Laboratories, Inc. (Knoxville, TN) using inductively coupled plasma-mass spectrometry (ICP-OES) for Gd. The Bio-Rad gel filtration standard used to compare the molecular weight of the antibody-dendrimer conjugate was purchased from Bio-Rad (Hercules, CA). The tris(2-carboxyethyl)phosphine hydrochloride (TCEP)

disulfide reducing gel (8  $\mu$ moles per mL gel) and sulfosuccinimidyl 4-[*N*-maleimidomethyl]cyclohexane-1-carboxylate (sulfo-SMCC) were purchased from Thermo Scientific (Rockford, IL). An Agilent 8453 UV-Visible spectrophotometer (Agilent Technologies; Foster City, CA) was employed to generate a standard curve. A Beckman Allegra™ 21R Centrifuge (Fullerton, CA) along with Amicon® Bioseparations Centricon® filters (MWCO 50,000) was used to purify the antibody-dendrimer conjugates. Preparation and characterization of the C-DOTA-Gd (**1**) was performed as previously reported.<sup>26</sup>

### Conjugation of G4SS and G5SS with **1** - (G4SS-(C-DOTA-Gd)<sub>30</sub>, G5SS-(C-DOTA-Gd)<sub>58</sub>)

These compounds were prepared following the procedure to prepare conjugates with ethylenediamine core dendrimer as previously reported (Figure 1);<sup>27</sup> 55% and 50 % yield for G4SS and G5SS, respectively, based on dendrimer). SE-HPLC  $t_R$  = 10.4 (G4SS-(C-DOTA-Gd)<sub>30</sub>; G4SS30 from this point on). Calcd for C<sub>624</sub>H<sub>1252</sub>N<sub>250</sub>O<sub>124</sub>S<sub>2</sub>·30(C<sub>24</sub>H<sub>30</sub>N<sub>5</sub>SO<sub>8</sub>Gd)·51(Na)·55(H<sub>2</sub>O): 42.89 (C), 6.31 (H), 15.08 (N), 2.47 (S), 12.16(Gd). Found: 42.93, 6.19, 15.19, 2.52, 11.96. SE-HPLC  $t_R$  = 9.2 (G5SS-(C-DOTA-Gd)<sub>58</sub>; G5SS58 from this point on). Calcd for C<sub>1264</sub>H<sub>2528</sub>N<sub>506</sub>O<sub>252</sub>S<sub>2</sub>·58(C<sub>24</sub>H<sub>30</sub>N<sub>5</sub>SO<sub>8</sub>Gd)·45(Na)·50(H<sub>2</sub>O): 44.43 (C), 6.31 (H), 15.48 (N), 2.67 (S), 12.67(Gd). Found: 44.31, 6.15, 15.65, 2.45, 12.89.

### Conjugation of F(ab')<sub>2</sub> with Sulfo-SMCC

A literature procedure was followed with a brief modification (Figure 2).<sup>17</sup> Sulfo-SMCC (80  $\mu$ L of 25 mg/mL, 4.6  $\mu$ mol) solution prepared in water/DMF (1:1) (with gentle warming) was added to 1 mL of 5 mg/mL (0.063  $\mu$ mol) antibody solution in PBS and the mixture was incubated for 4 h at room temperature. The F(ab')<sub>2</sub>-SMCC conjugate was purified by a Sephadex G-100 column. The amount of antibody was determined by Lowry assay<sup>28</sup> where the maleimide (SMCC) was determined by Ellman's and Cysteine assay.<sup>29</sup> The number of maleimide functions per F(ab')<sub>2</sub> molecule was found to be 4.3. SE-HPLC  $t_R$  = 9.4.

### Conjugation of F(ab')<sub>2</sub>-SMCC with reduced dendrimers- Ab-G4S15, Ab-G5S29

**G4SS30** (0.015 g) or **G5SS58** (0.029 g) (0.40  $\mu$ mol) in 800  $\mu$ L of water was reacted with 200  $\mu$ L (1.6  $\mu$ mol) of TCEP gel solution at room temperature for 3 h and directly filtered into the solutions of antibody-SMCC (1:4) using a syringe tip filter (0.22  $\mu$ m). The mixed solutions were incubated at room temperature for 3.5 h. The F(ab')<sub>2</sub>-dendrimer was purified by spin filtration (50,000 MCO). The filtration process was repeated using PBS until the filtrate was clear. The SE-HPLC retention time were 9.2 and 8.8 min for Ab-(G4S15)<sub>4</sub> and Ab-(G5S29)<sub>4</sub> respectively. It has been noted that the dendrimer moiety interferes with the Lowry assay, which limits the determination of antibody content in dendrimer-antibody solution. Therefore, to obtain the concentration of antibody in the purified F(ab')<sub>2</sub>-dendrimer- conjugate, the change in volume of F(ab')<sub>2</sub> antibody solution before and after conjugation to the dendrimer was followed since the concentration of antibody solution before conjugation was known.

### Molar Relaxivity Measurements

Solutions of [Gd(DTPA)]<sup>-2</sup> used as a reference standard (Magnevist™; Bayer, Montville, NJ) at 0.25, 0.50, 0.75, 1.0 and 2.0 mM, and 0.1, 0.25, 0.50, 0.75 and 1.0 mM of the four agents were prepared in PBS (300  $\mu$ L). Relaxivity measurements were obtained at ~22°C using a 3-Tesla clinical scanner (Signa Excite, GE Medical System, Waukesha, WI) equipped with a human knee coil (GE Medical System, Waukesha, WI). A series of variable TR single slice 2D spin echo images of all the solutions were acquired at the same time with a TE around 9 ms and using different repetition times (TR = 100, 350, 750, 1250, 2500, and 5000 ms). The R<sub>1</sub> map was calculated from variable TR SE images in ImageJ

(<http://rsb.info.nih.gov/ij>) using the MRI analysis plug-in (<http://rsb.info.nih.gov/ij/plugins/mri-analysis.html>). The molar relaxivity,  $r_1$ , was obtained from the slope of  $1/T_1$  vs.  $[\text{Gd(III)}]$  plots determined from region of interest measurements.

### **In Vivo Magnetic Resonance Imaging (MRI)**

All animal studies were performed in accordance with the NIH guidelines for the humane use of animals and all procedures were reviewed and approved by the National Cancer Institute Animal Care and Use Committee. Normal 6-10 week old female nude mice (NCI-Frederick, Frederick, MD) were imaged in pairs to increase throughput using a 3T clinical scanner (Signa Excite) equipped with a human knee coil (GE Medical System). Each mouse was anesthetized using gas mixtures of 3% isoflurane in  $\text{O}_2$ , and a catheter line (27 gauge needle on a 0.010" ID  $\times$  24" long Tygon tubing) filled with PBS was inserted into the tail vein. The mouse was then carefully placed in a mouse bed equipped with a nose cone and a water pad which was heated to maintain the mice at 34°C and positioned in the human knee coil. After acquiring a tri-planar gradient echo survey, a coronal view  $T_1$ -weighted 3D-fast spoiled gradient echo image with a low flip angle (repetition time of 10 ms, echo time of 3.3 ms, flip angle of 4°, field of view of 160  $\times$  63 mm, matrix size of 512  $\times$  256 pixels, 80 slices, slice thickness of 0.6 mm and 1 average; scan time of 2.3 min) was acquired. This was then followed by a dynamic series using a higher flip angle of 30° and 4 averages repeated every 3.2 min for 60 min. The contrast agent was injected (50  $\mu\text{L}$  of solution in PBS based on Gd(III) and pushed with 150  $\mu\text{L}$  of PBS) after the first dynamic image. The injection doses were 15-50  $\mu\text{mol/kg}$ . Blood clearance rates were determined from ROI intensity measurements of the jugular vein in the dynamic images using ImageJ. The intensity values during the dynamic scans were then converted to Gd(III) concentration and the resulting [Gd] time curves were fitted to a single exponential function using an Igor Pro (Wavemetrics) macro.

### **Relaxometry**

Relaxation measurements were made on a custom designed variable field  $T_1$ - $T_2$  analyzer (Southwest Research Institute, San Antonio, TX) at 23°C and 1mM solution in PBS. The field strength was varied from 0.02 to 1.5 T (1–64 MHz).  $T_1$  was measured using a saturation recovery pulse sequence with 32 incremental recovery times. The relaxivities (relaxation rates per mM concentration of metal ion) were obtained after subtracting the buffer (PBS, 0.01 M phosphate, 0.01 M NaCl, pH 7.4) contribution.

### **Photon correlation spectroscopy (PCS) and Zeta ( $\zeta$ ) potential**

Photon correlation spectroscopy (PCS) was used to determine the size of particles in solution in the submicron range ( $> 3$  nm).<sup>30-31</sup> PCS measurements were performed with a Zetasizer Nano ZS (Malvern, Worcestershire, United Kingdom) with a fixed 173° scattering angle and external fiber angle, and a 633-nm helium-neon laser. Data were analyzed using the associated Zetasizer software (Dispersion Technology Software 4.2; Malvern). The size and zeta potential of conjugates determined here is based on 1 mM (based on  $\text{Gd}^{3+}$ ). Solutions containing dendrimer and antibody (diluted from stock solution in PBS) were prepared in double-deionized water (pH ~6.0) and PCS measurements were recorded 30 to 40 minutes after sample preparation. The  $\zeta$  potential of the solutions was measured using the Zetasizer Nano ZS using a disposable clear cuvette. The determination of the  $\zeta$  potential is based on a measure of the electrophoretic mobility of particles under an applied electric field.

## Results and Discussion

The *C*-DOTA (2-(4-nitrobenzyl)-1,4,7,10-tetraazacyclododecane-*N,N',N'',N'''*-tetraacetic acid) ligand is first used to sequester Gd(III) and thereafter the formed metal complex is covalently attached to the terminal  $-\text{NH}_2$  groups of the cystamine core dendrimers (Figure 1) as previously reported.<sup>26-27, 32-33</sup> Herein, the approach was extended to the preparation of antibody based agents with the ultimate goal of utilizing them for target-specific imaging agents. The presence of a cleavable disulfide bond in a cystamine core dendrimer provides a unique orthogonal building block site to assemble an antibody-dendrimer conjugate. The studies described herein also take advantage of a well-established method in which an antibody is functionalized with a thiol-reactive maleimide group. Immobilized TCEP disulfide reducing gel was chosen to reduce the cystamine core dendrimer mainly because it is convenient to remove from the reduced dendrimer through filtration while other reducing agents such as dithiothreitol (DTT) require exhaustive dialysis. Sulfo-SMCC was used to functionalize the panitumumab  $\text{F}(\text{ab}')_2$ , and then conjugated to the reduced dendrimer with quantitative yield.

The two dendrimer conjugates were purified by a Sephadex-G50 column eluted with pure water (pH~7.5) which is also utilized by other researchers.<sup>34</sup> The  $\text{F}(\text{ab}')_2$ -dendrimer conjugates on the other hand were purified by spin-filtration and exchanging them into PBS solution. The solutions prepared for *in vitro* and *in vivo* studies were based on the gadolinium content from the ICP report and also from acid digestion<sup>35</sup> of the purified dendrimer conjugate. The  $\text{F}(\text{ab}')_2$  content was determined by a Lowry assay<sup>28</sup> while the content of maleimide on the  $\text{F}(\text{ab}')_2$  was determined by cysteine and Ellman's assay<sup>29</sup> after conjugation to the SMCC, which resulted in four maleimide (SMCC) per antibody molecule. The change in volume of known concentration of the antibody before and after conjugation to the dendrimer was used to determine the concentration of the antibody in the purified Ab-Den conjugates since the dendrimer interferes with the Lowry assay. HPLC data showed that the mAb-Dendrimer (Ab-Den from this point on) conjugates were stable for greater than a month.

Figure 3 shows a plot of the inverse longitudinal relaxation time ( $1/T_1$ ) versus Gd(III) concentration for Magnevist<sup>TM</sup> (0.25-2 mM), G4SS30, G5SS58, Ab-(G4S15)<sub>4</sub> and Ab-(G5S29)<sub>4</sub> (0.1-1 mM) while the relaxivity values obtained as a slope of this plot are summarized in Table 1. The data showed that the relaxivity of the two dendrimer agents are 4-7 times higher than Magnevist<sup>TM</sup> while the two Ab-Den agents, which have lower number of chelates, have a lesser impact (1.5-3). This is in line with our previous observation where the relaxivity is dependent on the number of chelated Gd(III) ions.<sup>32</sup> Figure 4 showed the  $1/T_1$  NMRD profiles of the four agents, wherein the relaxivity peaked between 17 and 27 MHz. These values are well within the range of the field strength of clinical MRI instrumentations (2-180 MHz). This behavior is similar to previously reported measurement using dendrimer- and albumin-based agents.<sup>26, 32, 36-37</sup>

The relaxivity values ( $6.7 \text{ mM}^{-1}\text{s}^{-1}$ ) reported here produced by Ab-(G4S15)<sub>4</sub> measured at 3T field is moderately higher than Magnevist<sup>TM</sup> ( $4.1 \text{ mM}^{-1}\text{s}^{-1}$ ) which has a single Gd(III) ion per molecule. The effect of the macromolecular antibody conjugates on proton relaxation enhancement is similar to that of the small molecule. Similar behavior of an antibody conjugate producing such a low rate of enhancement has been reported earlier.<sup>38</sup> The strategy of these studies was to employ higher generation cystamine core dendrimers, such as 6 or 7, to increase the relaxivity of the Ab-Den assembly since it will contain not only a larger number of chelated Gd(III) ions, but also be of greater overall molecular weight and size. This indicates that pure dendrimer conjugates are more suitable and applicable for magnetic resonance angiography in the submicromolar range and thus also presents a higher



possibility of eliminating concerns regarding Gd(III) toxicity. Curtet et al. has pointed out that although the mAb itself has no paramagnetic effect, higher concentrations of mAb in mAb-Gd conjugates leads to higher proton relaxation time.<sup>39</sup> More studies are required to confirm such claims.

The low impact on water relaxation here might be the effect of a charged protein, i.e., antibody, on the water exchange kinetics as speculated in earlier reports from this laboratory since the measured relaxivity of Ab-Den agents are similar to the other protein-based agents (albumin).<sup>32</sup> The anionic carboxylate moieties or other functional groups might coordinate to the metal ion and replace or block bound water molecules, or the bulky antibody might hinder the water path and reduce availability of second sphere water molecules. This is contrary to what was observed for dendrimer conjugates where higher molecular weight compounds have a higher impact on the proton relaxation enhancement.<sup>40-41</sup> Relaxivity was observed to be linearly correlated to the number of conjugated chelates; the greater the number of chelates, the greater the relaxivity.<sup>32</sup> This indicates that the size, molecular weight and the number of chelates are all important parameters that impact water proton relaxation.

The data in Table 1 also compares the half-life and rates of clearance obtained from a single exponential decay fit of dendrimer and Ab-Den agents. The rate of clearance of G4SS30 is slightly higher than G5SS58, which is expected since the latter is larger with greater numbers of Gd(III). A decrease in the rate of clearance was also observed for both antibody-based agents as compared to free dendrimers. This is in line with the notion that large molecules have a slower rate of clearance. The hypothesis is that the agents were cleared mainly through the liver except for G4SS30, which was cleared via the kidneys. Overall, G4SS30 has the fastest rate of clearance and thus the shortest half-life, which is expected for the smallest agent. Compared to the ethylenediamine core dendrimers both cystamine core dendrimers in this report have a lower relaxivity (29.6 vs. 16.4 mM<sup>-1</sup>s<sup>-1</sup> for generation four), a shorter half-life (16.2 vs. 12.5 min for generation four) and a faster rate of clearance (0.06 vs. 0.08 min<sup>-1</sup> for generation four),<sup>26-27</sup> which has also been observed by other authors.<sup>6, 42-43</sup> The core effect of the dendrimer as well as the interior architecture functionality are yet additional parameters to consider in designing more efficient MRI agents.

The dynamic contrast-enhanced MR images shown in Figure 5 illustrate differences in the circulation properties of the macromolecular agents. The signal intensity in the kidneys gradually increased 4 min after injection of the G4SS30 due to the high blood flow through this area and fast clearance of the agent. The G5SS58 agent allowed a clearer and finer visualization of the blood vessels, as well as higher signal intensity in the cranial region as compared to the others, which could be useful as a brain imaging agent. The fact that the G4SS30 and the two antibody-based agents did not produce similar images in cranial region might indicate the effect and contribution of molecular weight and size in permeating the blood brain barrier (BBB).

Figure 6 and Table 1 show the impact of the antibody fragment on the blood pharmacokinetics. The blood clearance half-lives reported here for G5SS58 along with the two antibody based agents are based on the first faster portion ( $T_{1/2\alpha}$ ) of the biphasic clearance. This is consistent with other reports in the literature.<sup>26, 44</sup> The  $T_{1/2\beta}$  was impossible to measure due to the time restraint of maintaining the mice under anesthesia during the MRI session. The full blood clearance profiles can be achieved by labeling the agents with radioactive gadolinium (<sup>153</sup>Gd), a study which is planned in the near future with the larger Ab-Den agents that will be prepared following the same procedure as reported here.

A comprehensive study further characterizing the F(ab')<sub>2</sub>-dendrimer conjugates reported here, including assessing the effect of the dendrimer, on immunoreactivity, is also underway. Mier et al pointed out through their study that the number of derivatization sites on an antibody, either by dendrimers modified with small chelates or just small chelates itself, not the size, has a significant effect on the immunoreactivity of the antibody.<sup>17</sup> Such studies are requisite for clinical translation of such agents.

In the studies reported here, the half-life values increased for both dendrimers following conjugation to the panitumumab F(ab')<sub>2</sub>, an outcome that was not unexpected. This result is most likely due to the increase in the molecular weight and size of the combined agents (Table 2). As previously noted, larger agents have a slower clearance. Another probable explanation for this is that the antibody-based agents might have an overall negative charge mainly from charged functional groups present in proteins, in this case, the antibody fragment. High negatively charged agents also characteristically have slower blood clearance half-lives.<sup>33</sup>

The data in Table 2 compares molecular weights, sizes, and the  $\zeta$  potentials of the five agents along with the antibody fragment. The size and  $\zeta$  potential determined here is based on a 1 mM (based on Gd<sup>3+</sup>) solution prepared in ambient water at pH = 6 similar to what was previously used for the dendrimer conjugates (Table 2).<sup>32</sup> This is to eliminate buffer interference as size measurement based on photon correlation spectroscopy (PCS) is sensitive to both concentration,<sup>30</sup> and to buffer.<sup>45</sup> As expected, the Ab-(G5S29)<sub>4</sub> conjugate was found to have the largest size and molecular weight (Table 2). However, contrary to our previous observation, its impact on proton relaxation is rather low as compared to the pure dendrimer (Table 1),<sup>26</sup> a result

Zeta potential ( $\zeta$ ) indicates the accumulation of ions at the particle surface.<sup>30</sup> The data suggest that the overall surface charge or  $\zeta$  potential of the G5SS58 agent is the highest, as expected, due to the highest density of surface charge (Table 2). Also, high positive or negative potential is indicative of high electrostatic repulsion between particles and provides an energy barrier against aggregation.<sup>30</sup> The  $\zeta$  potentials of the two antibody-based conjugates are about the same, but lower than that of the dendrimer conjugates and slightly higher than pure antibody. Again, this might be due to the presence of charged functional groups at the surface of the antibody fragment. All of the agents have negative  $\zeta$  potential (16-43) based on the data obtained, indicating there to be a decreased likelihood of each agent to aggregate. This is advantageous especially for *in vivo* applications where aggregation could interfere with glomerular filtration renal clearance, the preferred excretion route.<sup>46</sup>

In summary, the appending of a dendrimer or dendron to an antibody fragment has been demonstrated. This technique provides insight into how to produce antibody-dendrimer conjugates with differing sizes of dendrimer using a SMCC bridge. This study indicates that antibody based MRI contrast agents may be useful as blood pool agents. However, our ultimate goal of making antibody-dendrimer conjugate is for target specific delivery of the imaging agent. Tumor imaging studies are underway to demonstrate the *in vivo* viability of these agents. This study also shows that macromolecular MRI contrast agents composed of multiple Gd(III) chelates assembled on a dendrimer platform are much more efficient and effective in modulating and relaxing water protons as compared to a single chelate unit analogue.

## Acknowledgments

This research was supported by the Intramural Research Program of the National Institute of Health, National Cancer Institute, Center for Cancer Research and the United States Department of Health and Human Services. We

thank Dr. L. Henry Bryant, Jr., Laboratory of Diagnostic Radiology Research (LDRR), National Institute of Health, for his help with the instrumentation for photon correlation spectroscopy (PCS).

## References

1. Caravan P. Strategies for increasing the sensitivity of gadolinium based MRI contrast agents. *Chem. Soc. Rev.* 2006; 35:512–523. [PubMed: 16729145]
2. Wang SJ, Brechbiel M, Wiener EC. Characteristics of a New MRI Contrast Agent Prepared From Polypropyleneimine Dendrimers, Generation 2. *Invest. Radiol.* 2003; 38:662–668. [PubMed: 14501494]
3. Koenig SH, Brown III RD. Relaxation of solvent protons by paramagnetic ions and its dependence on magnetic field and chemical environment: implications for NMR imaging. *Magn. Reson. Med.* 1984; 1:478–495. [PubMed: 6571571]
4. Koyama Y, Talanov VS, Bernardo M, Hama Y, Regino CAS, Brechbiel MW, Choyke PL, Kobayashi H. A dendrimer-based nanosized contrast agent dual-labeled for magnetic resonance and optical fluorescence imaging to localize the sentinel lymph node in mice. *J. Magn. Reson. Imaging.* 2007; 25:866–871. [PubMed: 17345640]
5. Sato N, Kobayashi H, Hiraga A, Saga T, Togashi K, Konishi J, Brechbiel MW. Pharmacokinetics and enhancement patterns of macromolecular MR contrast agents with various sizes of polyamidoamine dendrimer cores. *Magn. Reson. Med.* 2001; 46:1169–1173. [PubMed: 11746584]
6. Kobayashi H, Kawamoto S, Jo S-K, Bryant HL, Brechbiel MW, Star RA. Macromolecular MRI Contrast Agents with Small Dendrimers: Pharmacokinetic Differences between Sizes and Cores. *Bioconjugate Chem.* 2003; 14:388–394.
7. Bourne MW, Margerun L, Hylton N, Campion B, Lai J-J, Derugin N, Higgins CB. Evaluation of the effects of intravascular MR contrast media (gadolinium dendrimer) on 3D time of flight magnetic resonance angiography of the body. *J. Magn. Reson. Imaging.* 1996; 6:305–310.
8. Erik W, Brechbiel MW, Brothers H, Magin RL, Gansow OA, Tomalia DA, Lauterbur PC. Dendrimer-based metal chelates: A new class of magnetic resonance imaging contrast agents. *Magn. Reson. Med.* 1994; 31:1–8. [PubMed: 8121264]
9. Tomalia DA, Reyna LA, Svenson S. Dendrimers as multi-purpose nanodevices for oncology drug delivery and diagnostic imaging. *Biochem. Soc. Trans.* 2007; 035:61–67. [PubMed: 17233602]
10. Barth RF, Adams DM, Soloway AH, Alam F, Darby MV. Boronated starburst dendrimer-monoclonal antibody immunoconjugates: Evaluation as a potential delivery system for neutron capture therapy. *Bioconjugate Chem.* 1994; 5:58–66.
11. Kobayashi H, Wu C, Kim M-K, Paik CH, Carrasquillo JA, Brechbiel MW. Evaluation of the in Vivo Biodistribution of Indium-111 and Yttrium-88 Labeled Dendrimer-1B4M-DTPA and Its Conjugation with Anti-Tac Monoclonal Antibody. *Bioconjugate Chem.* 1998; 10:103–111.
12. Singh P, Moll F 3rd, Lin SH, Ferzli C, Yu KS, Koski RK, Saul RG, Cronin P. Starburst dendrimers: enhanced performance and flexibility for immunoassays. *Clin. Chem.* 1994; 40:1845–1849. [PubMed: 8070111]
13. Wu C, Brechbiel MW, Kozak RW, Gansow OA. Metal-chelate-dendrimer-antibody constructs for use in radioimmunotherapy and imaging. *Bioorg. Med. Chem. Lett.* 1994; 4:449–454.
14. Wu G, Barth RF, Yang W, Kawabata S, Zhang L, Green-Church K. Targeted delivery of methotrexate to epidermal growth factor receptor-positive brain tumors by means of cetuximab (IMC-C225) dendrimer bioconjugates. *Mol. Cancer Ther.* 2006; 5:52–59. [PubMed: 16432162]
15. Kobayashi H, Sato N, Saga T, Nakamoto Y, Ishimori T, Toyama S, Togashi K, Konishi J, Brechbiel MW. Monoclonal antibody-dendrimer conjugates enable radiolabeling of antibody with markedly high specific activity with minimal loss of immunoreactivity. *Eur. J. Nucl. Med. Mol. Imaging.* 2000; 27:1334–1339.
16. Wu G, Barth RF, Yang W, Chatterjee M, Tjarks W, Ciesielski MJ, Fenstermaker RA. Site-Specific Conjugation of Boron-Containing Dendrimers to Anti-EGF Receptor Monoclonal Antibody Cetuximab (IMC-C225) and Its Evaluation as a Potential Delivery Agent for Neutron Capture Therapy. *Bioconjugate Chem.* 2003; 15:185–194.



17. Wängler C, Moldenhauer G, Eisenhut M, Haberkorn U, Mier W. Antibody–Dendrimer Conjugates: The Number, Not the Size of the Dendrimers, Determines the Immunoreactivity. *Bioconjugate Chem.* 2008; 19:813–820.
18. Xu H, Regino CAS, Koyama Y, Hama Y, Gunn AJ, Bernardo M, Kobayashi H, Choyke PL, Brechbiel MW. Preparation and Preliminary Evaluation of a Biotin- Targeted, Lectin-Targeted Dendrimer-Based Probe for Dual-Modality Magnetic Resonance and Fluorescence Imaging. *Bioconjugate Chem.* 2007; 18:1474–1482.
19. Mano M, Humblet Y. Drug Insight: panitumumab, a human EGFR-targeted monoclonal antibody with promising clinical activity in colorectal cancer. *Nat. Clin. Prac. Oncol.* 2008; 5:415–425.
20. Wu M, Rivkin A, Pham T. Panitumumab: Human monoclonal antibody against epidermal growth factor receptors for the treatment of metastatic colorectal cancer. *Clin. Ther.* 2008; 30:14–30. [PubMed: 18343240]
21. Baselga J, Arteaga CL. Critical Update and Emerging Trends in Epidermal Growth Factor Receptor Targeting in Cancer. *J. Clin. Oncol.* 2005; 23:2445–2459. [PubMed: 15753456]
22. Ray GL, Baidoo KE, Wong KJ, Williams M, Garmestani K, Brechbiel MW, Milenic DE. Preclinical evaluation of a monoclonal antibody targeting the epidermal growth factor receptor as a radioimmunodiagnostic and radioimmunotherapeutic agent. *Br. J. Pharmacol.* 2009; 157:1541–1548. [PubMed: 19681874]
23. Wong K, Baidoo K, Nayak T, Garmestani K, Brechbiel M, Milenic D. In Vitro and In Vivo Pre-clinical Analysis of a F(ab')<sub>2</sub> Fragment of Panitumumab for Molecular Imaging and Therapy of HER1 Positive Cancers. *Eur. J. Nuc. Med. Mol Imaging Res.* 2011; 1:1–15.
24. Milenic DE, Yokota T, Filipula DR, Finkelman MAJ, Dodd SW, Wood JF, Whitlow M, Snoy P, Schlom J. Construction, Binding Properties, Metabolism, and Tumor Targeting of a Single-Chain Fv Derived from the Pancarcinoma Monoclonal Antibody CC49. *Cancer Res.* 1991; 51:6363–6371. [PubMed: 1933899]
25. Yokota T, Milenic DE, Whitlow M, Schlom J. Rapid Tumor Penetration of a Single-Chain Fv and Comparison with Other Immunoglobulin Forms. *Cancer Res.* 1992; 52:3402–3408. [PubMed: 1596900]
26. Nwe K, Bryant LH, Brechbiel MW. Poly(amidoamine) Dendrimer Based MRI Contrast Agents Exhibiting Enhanced Relaxivities Derived via Metal Preligation Techniques. *Bioconjugate Chem.* 2010; 21:1014–1017.
27. Nwe K, Bernardo M, Regino CAS, Williams M, Brechbiel MW. Comparison of MRI properties between derivatized DTPA and DOTA gadolinium–dendrimer conjugates. *Bioorg. Med. Chem.* 2010; 18:5925–5931. [PubMed: 20663676]
28. Lowry OH, Rosebrough NJ, Farr AL, Randall RJ. Protein measurement with the folin phenol reagent. *J. Biol. Chem.* 1951; 193:265. [PubMed: 14907713]
29. Singh R. A Sensitive Assay for Maleimide Groups. *Bioconjugate Chem.* 1994; 5:348–351.
30. Suvarna S, Espinasse B, Qi R, Lubica R, Poncz M, Cines DB, Wiesner MR, Arepally GM. Determinants of PF4/heparin immunogenicity. *Blood.* 2007; 110:4253–4260. [PubMed: 17848616]
31. William Wilson W. Light scattering as a diagnostic for protein crystal growth--A practical approach. *J. Struct. Biol.* 2003; 142:56–65. [PubMed: 12718919]
32. Nwe K, Milenic D, Bryant LH, Regino CAS, Brechbiel MW. Preparation, characterization and in vivo assessment of Gd-albumin and Gd-dendrimer conjugates as intravascular contrast-enhancing agents for MRI. *J. Inorg. Biochem.* 2011; 105:722–727. [PubMed: 21463567]
33. Nwe K, Xu H, Regino CAS, Bernardo M, Ileva L, Riffle L, Wong KJ, Brechbiel MW. A New Approach in the Preparation of Dendrimer-Based Bifunctional Diethylenetriaminepentaacetic Acid MR Contrast Agent Derivatives. *Bioconjugate Chem.* 2009; 20:1412–1418.
34. Neerman MF, Zhang W, Parrish AR, Simanek EE. In vitro and in vivo evaluation of a melamine dendrimer as a vehicle for drug delivery. *Int. J. Pharm.* 2004; 281:129–132. [PubMed: 15288350]
35. Barge A, Cravotto G, Gianolio E, Fedeli F. How to determine free Gd and free ligand in solution of Gd chelates. A technical note. *Contrast Media Mol. Imag.* 2006; 1:184–188.

36. Bryant LH Jr, Martin WB, Wu C, Bulte JWM, Herynek V, Frank JA. Synthesis and relaxometry of high-generation (G = 5, 7, 9, and 10) PAMAM dendrimer-DOTA-gadolinium chelates. *J. Magn. Reson. Imaging*. 1999; 9:348–352. [PubMed: 10077036]
37. Weiner EC, Brechbiel MW. Dendrimer-based metal chelates: a new class of magnetic resonance imaging contrast agents. *Magn. Reson. Med*. 1994; 31:1–8. [PubMed: 8121264]
38. Unger EC, Totty WG, Neufeld DM, Otsuka FL, Murphy WA, Welch MS, Connett JM, Philpott GW. Magnetic Resonance Imaging Using Gadolinium Labeled Monoclonal Antibody. *Invest. Radiol*. 1985; 20:693–700. [PubMed: 4066240]
39. Curtet C, Bourgoin C, Bohy J, Saccavini J-C, Thédrez P, Akoka S, Tellier C, Chatal J-F. Gd-25 DTPA-MAb, a potential NMR contrast agent for MRI in the xenografted nude mouse: Preliminary studies. *Int'l J. Cancer suppl*. 2. 1988; 41:126–132.
40. Kobayashi H, Sato N, Hiraga A, Saga T, Nakamoto Y, Ueda H, Konishi J, Togashi K, Brechbiel MW. 3D-micro-MR angiography of mice using macromolecular MR contrast agents with polyamidoamine dendrimer core with reference to their pharmacokinetic properties. *Magn. Reson. Med*. 2001; 45:454. [PubMed: 11241704]
41. Kobayashi H, Brechbiel MW. Dendrimer-based Macromolecular MRI Contrast Agents: Characteristics and Application. *Mol. Imaging*. 2003; 2:1–10. [PubMed: 12926232]
42. Kobayashi H, Brechbiel MW. Nano-sized MRI contrast agents with dendrimer cores. *Adv. Drug Deliv. Rev*. 2005; 57:2271–2286. [PubMed: 16290152]
43. Kobayashi H, Sato N, Kawamoto S, Saga T, Hiraga A, Haque TL, Ishimori T, Konishi J, Togashi K, Brechbiel MW. Comparison of the Macromolecular MR Contrast Agents with Ethylenediamine-Core versus Ammonia-Core Generation-6 Polyamidoamine Dendrimer. *Bioconjugate Chem*. 2000; 12:100–107.
44. Kobayashi H, Sato N, Hiraga A, Saga T, Nakamoto Y, Ueda H, Konishi J, Togashi K, Brechbiel MW. 3D-micro-MR angiography of mice using macromolecular MR contrast agents with polyamidoamine dendrimer core with reference to their pharmacokinetic properties. *Magn. Reson. Med*. 2001; 45:454–460. [PubMed: 11241704]
45. Margerum LD, Champion BK, Koo M, Shargill N, Lai J-J, Marumoto A, Christian Sontum P. Gadolinium(III) DO3A macrocycles and polyethylene glycol coupled to dendrimers Effect of molecular weight on physical and biological properties of macromolecular magnetic resonance imaging contrast agents. *J. Alloys Compd*. 1997; 249:185–190.
46. Vexler VS, Clément O, Schmitt-Willich H, Brasch RC. Effect of varying the molecular weight of the MR contrast agent Gd-DTPA-polylysine on blood pharmacokinetics and enhancement patterns. *J. Magn. Reson. Imaging*. 1994; 4:381. [PubMed: 8061437]

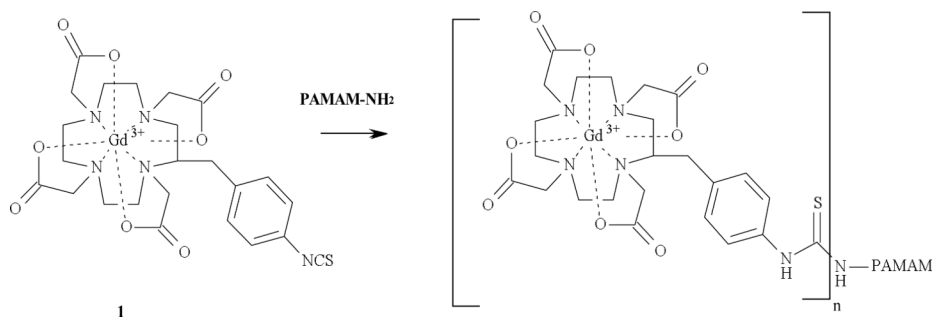


**Figure 1.**  
Conjugation of **1** to a dendrimer.

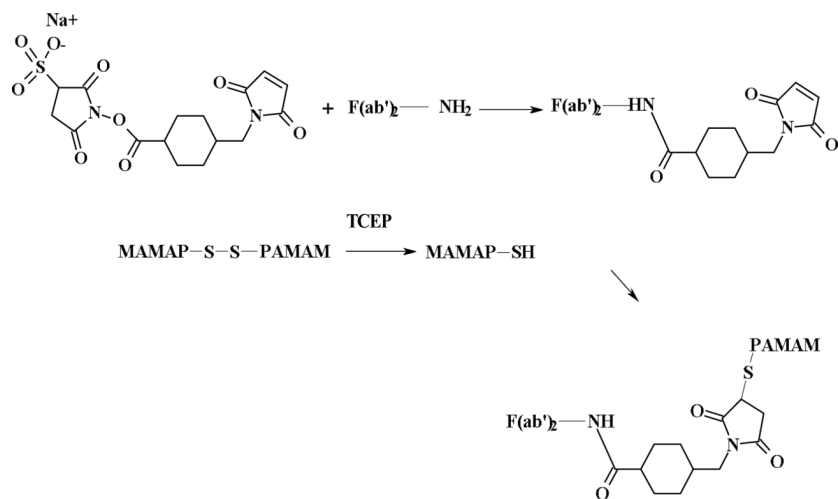


**Figure 2.**  
Conjugation of a mono-thiol half-dendrimer to F(ab')<sub>2</sub> of panitumumab.

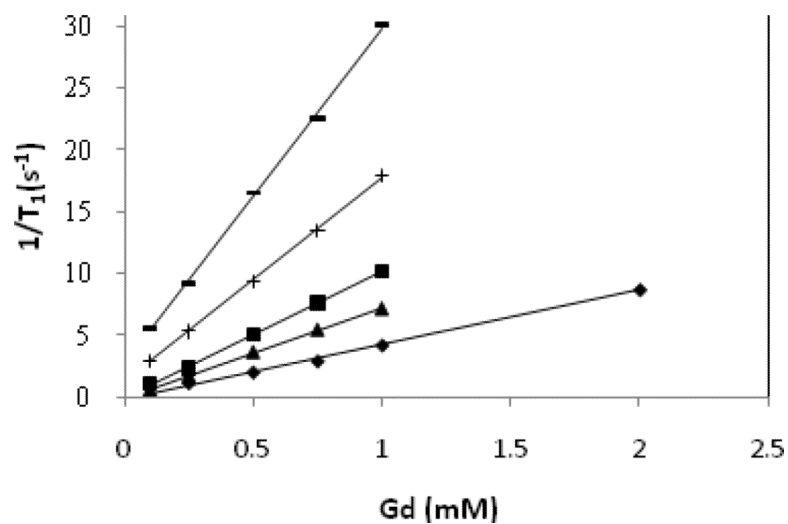


**Figure 3.** Molar relaxivity plot of Magnevist™ (◆; 4.1 mM<sup>-1</sup>s<sup>-1</sup>), Ab-(G4S15)<sub>4</sub> (▲; 6.7 mM<sup>-1</sup>s<sup>-1</sup>), Ab-(G5S29)<sub>4</sub> (■; 9.1 mM<sup>-1</sup>s<sup>-1</sup>), G4SS30 (+; 16.5 mM<sup>-1</sup>s<sup>-1</sup>), G5SS58 (-; 27.2 mM<sup>-1</sup>s<sup>-1</sup>) measured at room temperature and 3T.



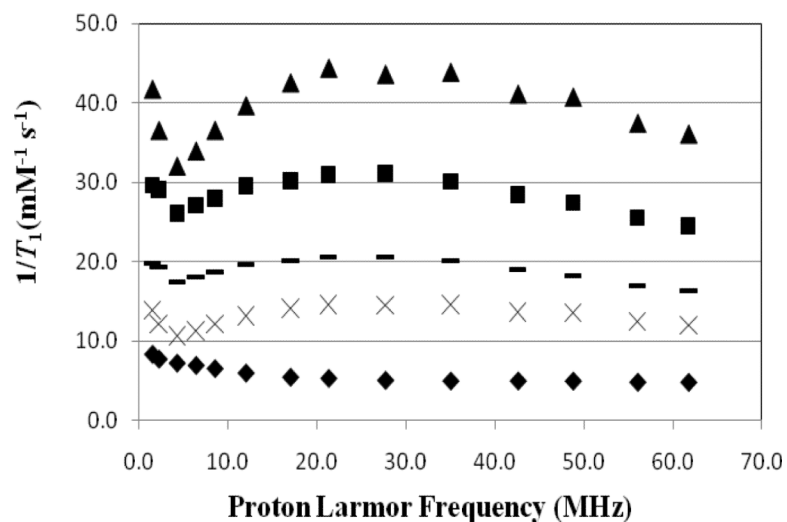
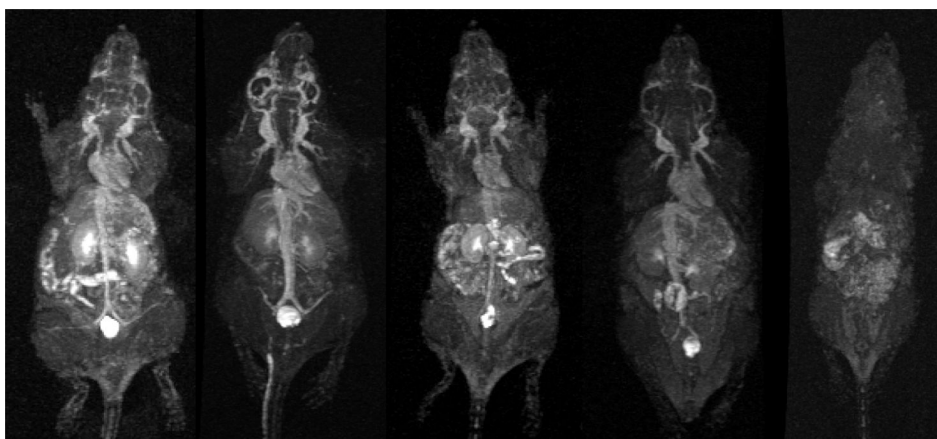


**Figure 4.** 1/T1 NMRD profiles of 1 mM solution of Magnevist® (◆), Ab-(G4S15)<sub>4</sub> (×), Ab-(G5S29)<sub>4</sub> (○), G4SS30 (■), G5SS58 (▲) as a function of frequencies at 23°C.



G4SS30      G5SS58      Ab-(G4S15)<sub>4</sub>      Ab-(G5S29)<sub>4</sub>      pre-injection

**Figure 5.** Dynamic MRI of mice injected with 0.015 mmol/kg of G4SS30 and G5SS58, and 0.050 mmol/kg of Ab-(G4S15)<sub>4</sub>, and 0.035 mmol/kg of Ab-(G5S29)<sub>4</sub>. All images were acquired at 12-16 min post injection. A pre-contrast image was included for comparison.

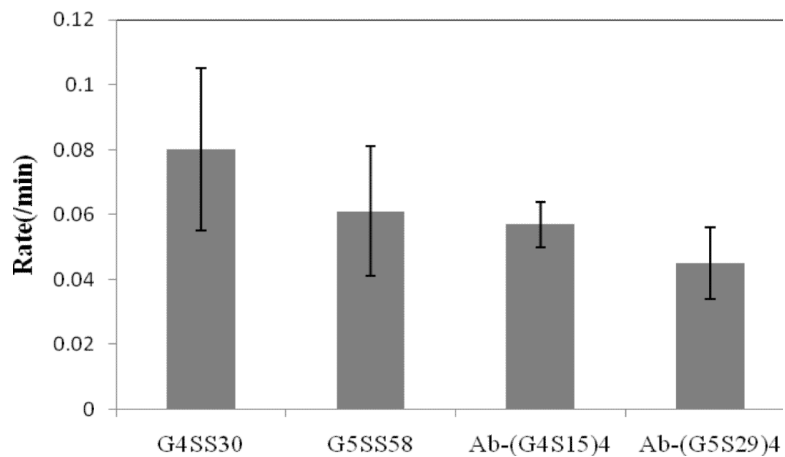


**Figure 6.** Average blood clearance rates measured at the jugular vein of G4SS30, G5SS58, Ab-(G4S15)<sub>4</sub> and Ab-(G5S29)<sub>4</sub>.

**Table 1**

Molar relaxivity, half-life and rate of clearance measured for dendrimers and antibody-dendrimer agents.

Agent	$r_1$ (mM <sup>-1</sup> s <sup>-1</sup> )	Half-life (min)	Rate of clearance (min <sup>-1</sup> )
Magnevist™	4.1 ± 0.5	---	---
G4SS30	16.4 ± 1.2	12.5 ± 3	0.080 ± 0.025
G5SS58	27.3 ± 1.4	16.3 ± 4	0.061 ± 0.020
Ab-(G4S15) <sub>4</sub>	6.7 ± 1.1	17.5 ± 3	0.057 ± 0.007
Ab-(G5S29) <sub>4</sub>	9.1 ± 1.3	22.2 ± 7	0.045 ± 0.011

**Table 2**Values of molecular weight, size and  $\zeta$  potential for the agents.

Agent	Molecular Weight	Measured Diameter (nm)	$\zeta$ Potential (eV)
G4SS30	37,631	4.7	-32
G5SS58	71,759	5.8	-43
Ab-(G4S15) <sub>4</sub>	155,262	9.3	-16
Ab-(G5S29) <sub>4</sub>	223,581	11.1	-20
Ab	80,000	7.8	-9